Inventory of Supplemental Information

The supplementary material includes five figures associated in order with Figures 1, 2, 3, 4, and 7 of the main manuscript. Supplementary text describing the brain innervation patterns in details. Supplementary experimental procedures for 4 commonly used techniques and supplementary references.

Melanopsin-expressing retinal ganglion-cell photoreceptors: cellular diversity and role in pattern vision.

Ecker et. al.

Table of Contents for Supplementary material

Supplementary Figures 2

Supplementary Text 12

Supplementary Experimental Procedures 15

Generation of the mouse models utilized in this study.....

Intracellular dye filling .....

Antibody Staining.....

OptoMotry .....

References..... 18

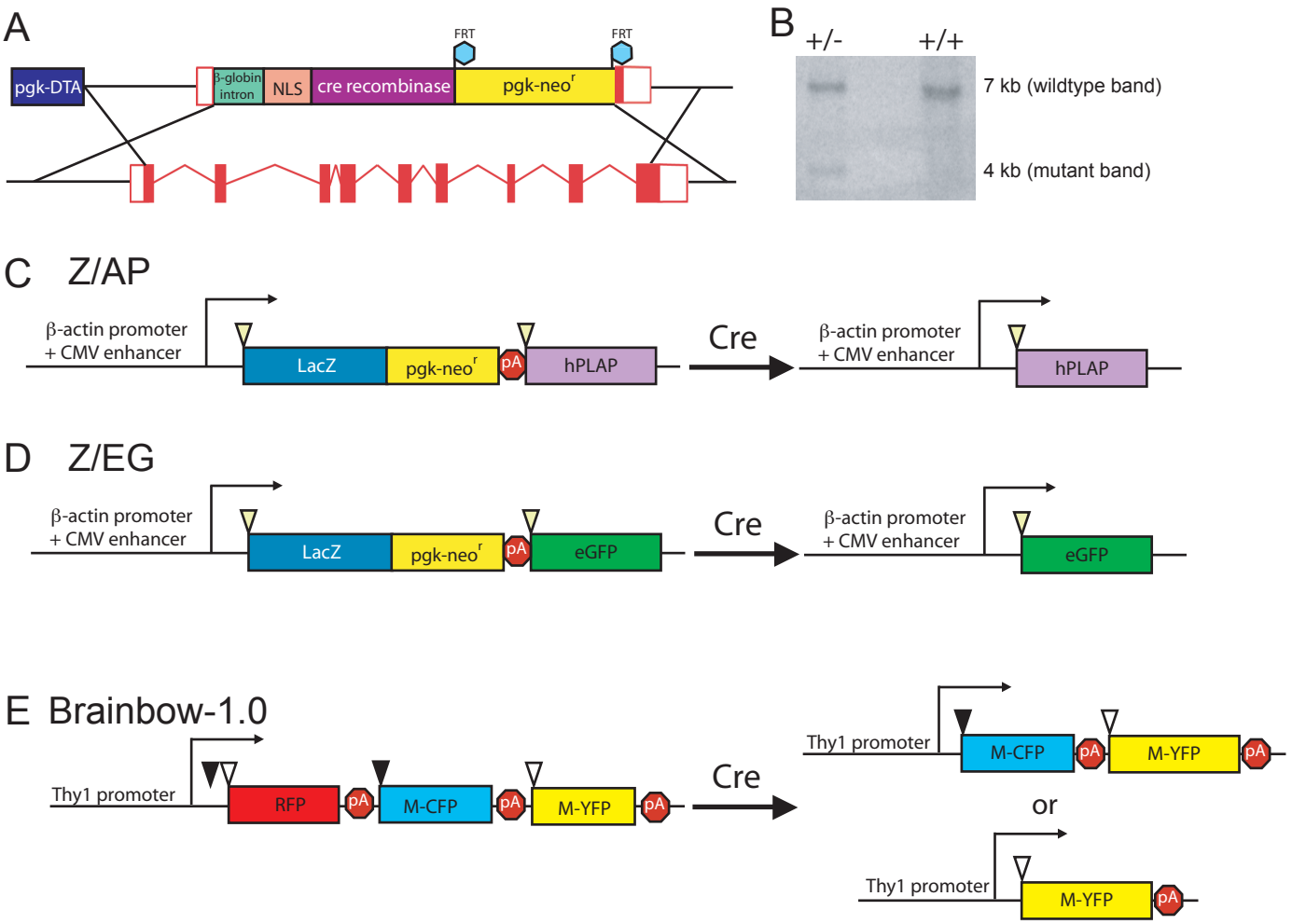

Ecker et al., Figure S1

Figure S1: Generation of melanopsin-Cre mice and reporter lines used for ipRGC labeling
(A) Targeting construct used to make *Opn4*^{Cre} mice, and method for insertion into the melanopsin locus (bottom, in red). (B) Southern blot hybridization showing proper genomic insertion of the construct. Heterozygous lane (left) shows successful recombination with wild type (7kb) and mutant (4kb) bands and wild type control lane (right) shows only the 7kb band. (C) Z/AP (Lobe et al., 1999) and (D) Z/EG (Novak et al., 2000) transgenes before recombination (left). In Cre-expressing cells (right), the LacZ-neomycin STOP cassette is excised, leading to the expression of human placental alkaline phosphatase (hPLAP) or enhanced green fluorescent protein (EGFP) driven by the β-actin promoter and CMV enhancer. (E) Before recombination, Brainbow-1.0 (Livet et al., 2007) expresses a cytoplasmic red fluorescent protein (RFP) and after recombination a membrane bound form of either cyan fluorescent protein (M-CFP) or yellow fluorescent protein (M-YFP) using the Thy-1 promoter. To visualize these reporter proteins by immunofluorescence, we used an anti-GFP antibody that recognizes CFP and YFP but not RFP.

M5

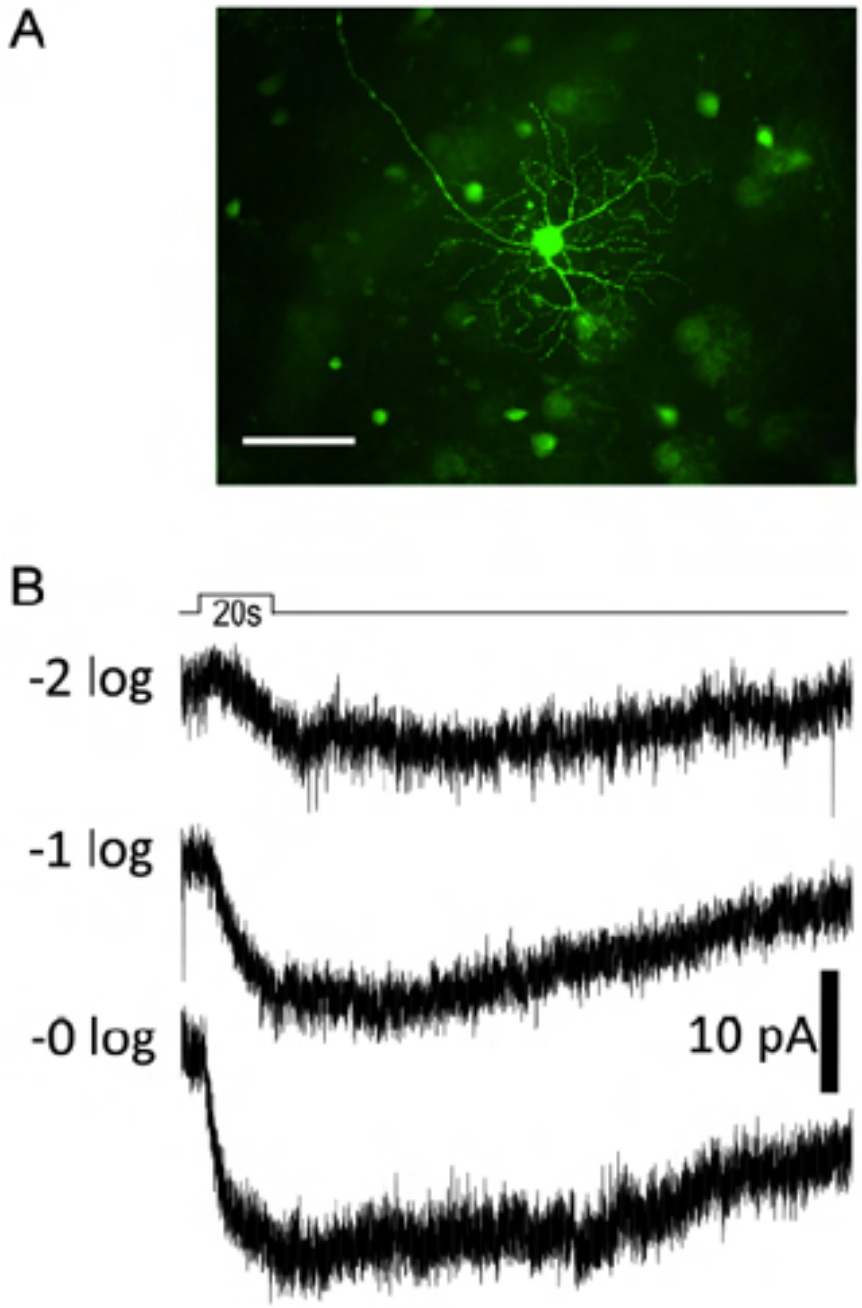

Ecker et al., Figure S2

Figure S2: Intrinsic light responses from a bushy-like "M5" ipRGC

(A) Neurobiotin fill of an EGFP-labeled ganglion cell from an *Opn4*$^{cre/+}$*;Z/EG* animal. (B) This cell was intrinsically photosensitive, as shown by the whole cell voltage clamp recordings, obtained during pharmacological blockade of retinal synapses. Each trace shows the response to a different light intensity. Values at left are the number of log units of attenuation in stimulus intensity from the maximal ("0 log"; 2.3×10^{13} photons cm^{-2} s^{-1}).

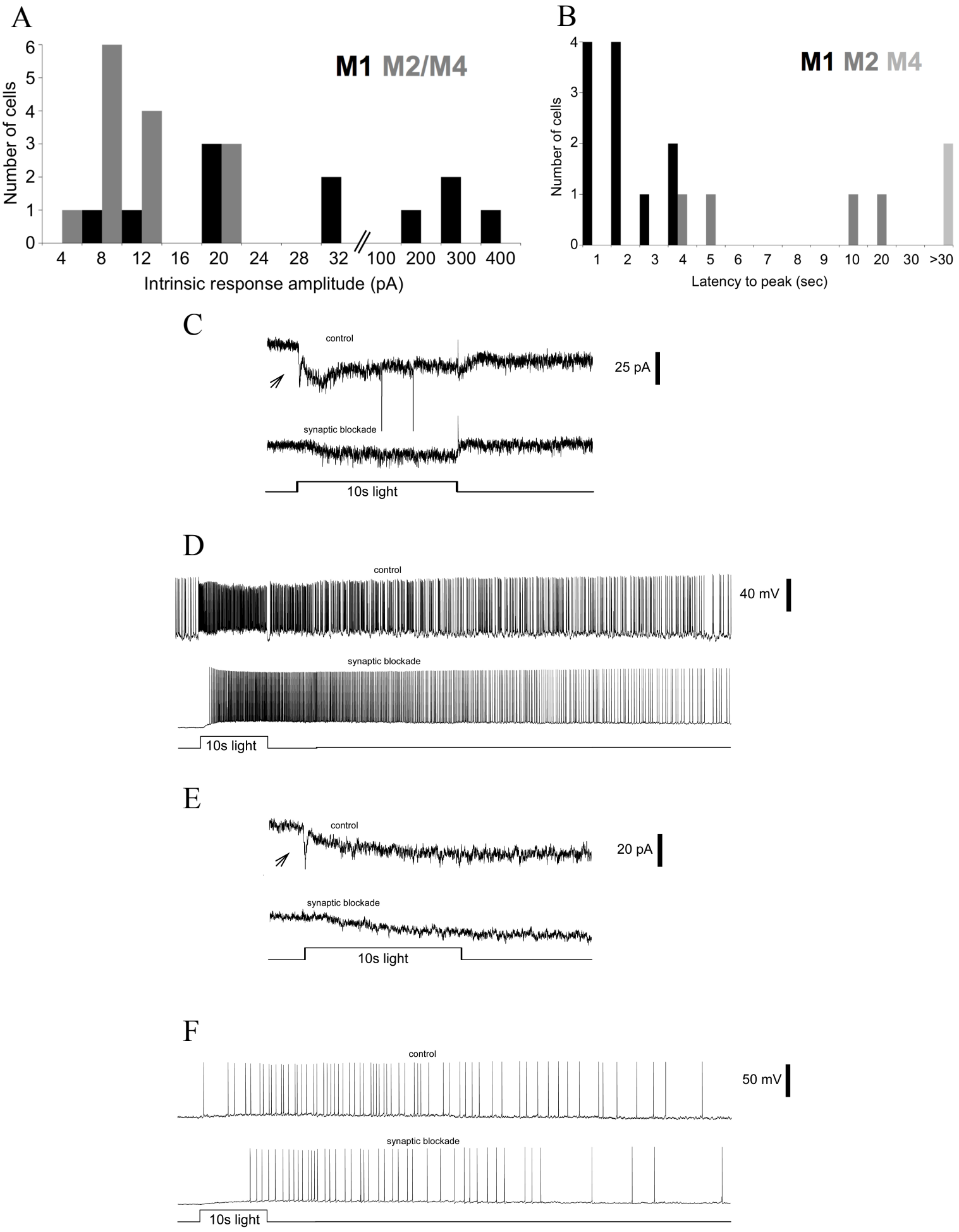

Ecker et al., Figure S3

Figure S3: Amplitude and latency of intrinsic light response of M2 and M4 ipRGCs compared to M1 subtype and their light-driven synaptic inputs

(A) Histogram of response amplitude, as measured by peak light-evoked currents. M1 ipRGCs (black bars) had the largest intrinsic light responses when compared to M2s and M4s, which are grouped together (gray bars). (B) Histogram of latency to peak of response, assessed at maximal irradiance ($2.3x10^{13}$ photons•cm^{-2}•sec^{-1}). M1 ipRGCs (black bars) exhibited the shortest latencies, M2 ipRGCs (gray bars) somewhat longer ones, and M4 ipRGCs (light gray bars) the slowest latencies, so slow that the response peak often occurred after stimulus offset. (C-F) Whole-cell recordings reveal that both M2 (C, D) and M4 ipRGCs (E, F) receive light-driven synaptic inputs that supplement their intrinsic photoresponses. Voltage-clamp recordings are shown in C (M2 cell) and E (M4 cell). Current clamp recordings from two different ipRGCs are shown in D (M2 cell) and F (M4 cell). In each panel, the upper trace shows the response to light (stimulus bar under trace) in control bathing solution, with synaptic transmission intact; the lower trace shows the same cell's response in the presence of antagonists that effectively block synaptic signaling to ipRGCs (100µM L-AP4, 40µM DNQX, and 30µM D-AP5; see Wong et al., 2007). Note that both M2 and M4 ipRGCs fire action potentials in response to light stimulation even under synaptic blockade. Fast downward deflections in middle of top trace in A are presumed action currents resulting from incomplete voltage clamp.

Opn4$^{cre/+}$; Z/AP - Enucleated

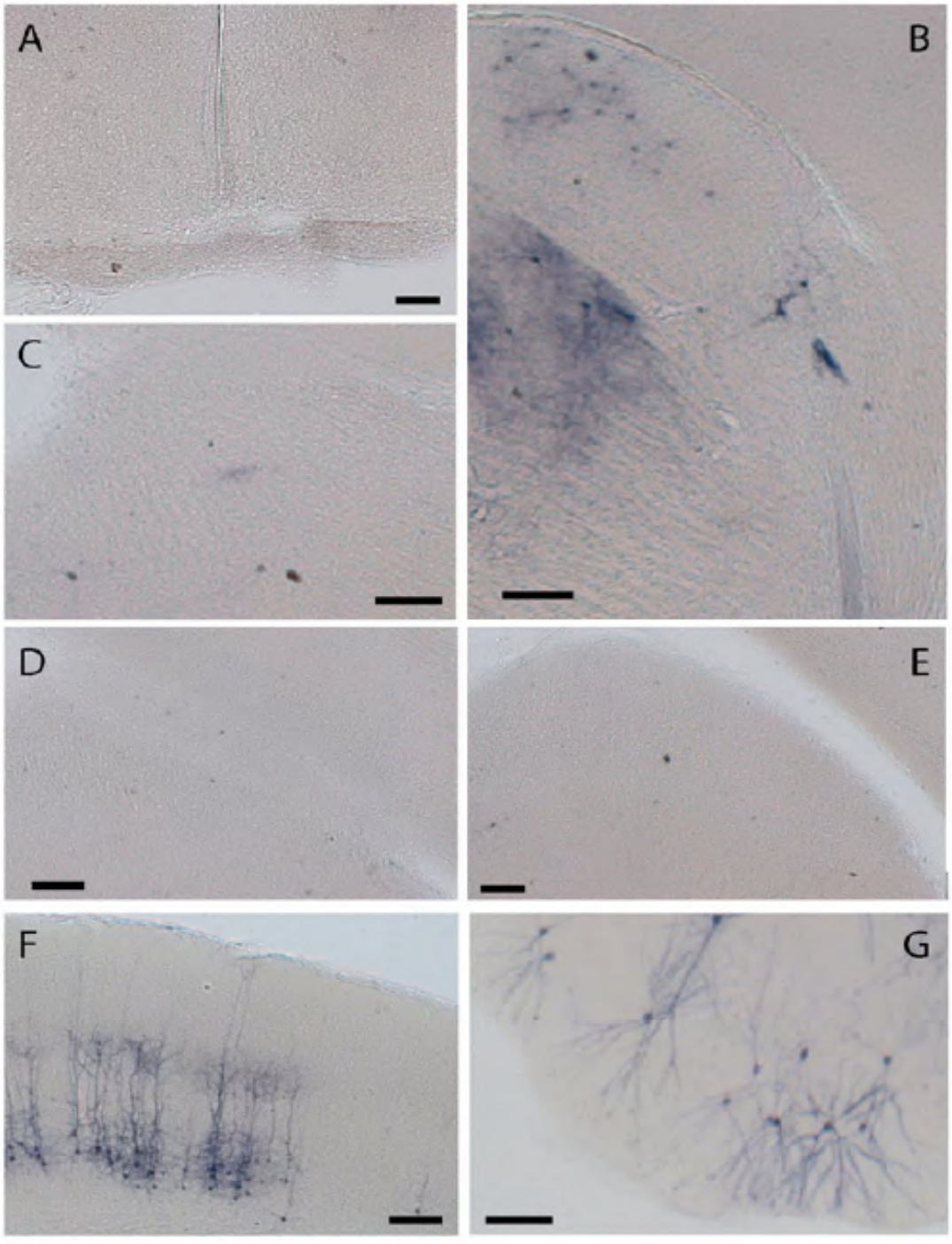

Ecker et al., Figure S4

Figure S4: Binocular eye removal eliminates alkaline-phosphatase-positive axons from visual nuclei in the *Opn4*$^{Cre/+}$; Z/AP brain

(A – E): Photomicrographs showing absence of alkaline phosphatase fiber labeling in retinorecipient brain nuclei in *Opn4*$^{Cre/+}$*; Z/AP* mice after destruction of retinal fibers by bilateral enucleation 3 weeks earlier. (A) suprachiasmatic nucleus, (B) lateral geniculate nucleus, (C) olivary pretectal nucleus, (D) posterior pretectal nucleus, (E) superior colliculus. In control animals, all of these nuclei exhibit strong fiber labeling (see Fig. 4, left panels). (F,G): Neocortical pyramidal cells (F) and neurons of the piriform cortex (G) remain labeled in enucleated animals, as in control mice. The thalamus also exhibits strong fiber labeling in the medial geniculate nucleus (B) and ventral posterior nucleus (not shown), presumably from labeled neurons in neocortex. Scattered neuronal cell bodies are also evident in the thalamus (B). Scale bars, 200 μm.

A

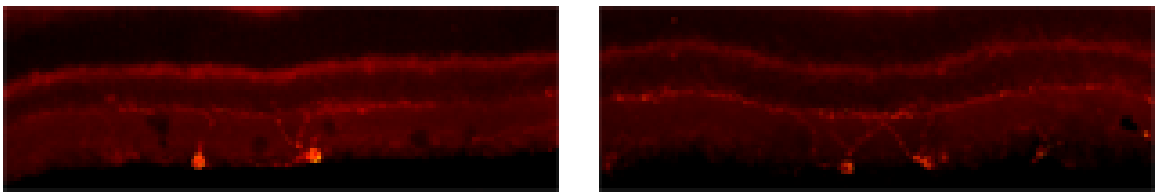

B

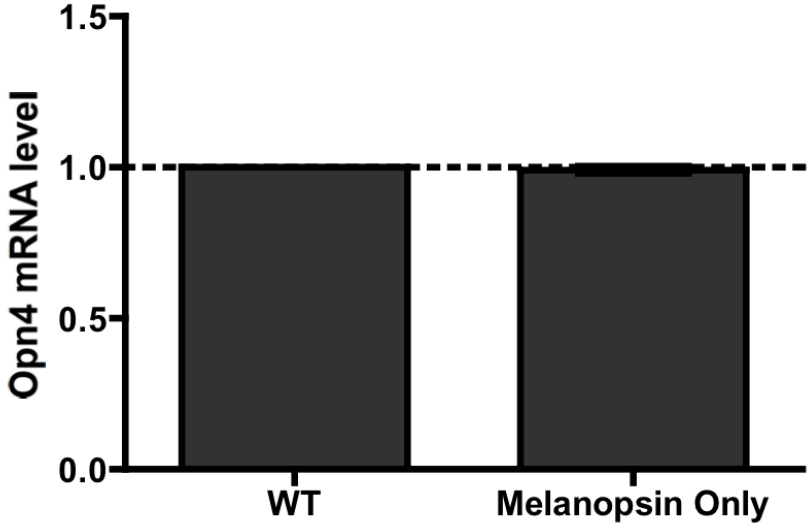

Ecker et al., Figure S5

Figure S5: Melanopsin expression and total mRNA amounts are similar in WT and MO animals

(A) Cross section of mouse retina showing that both WT and MO animals have the same staining pattern using melanopsin antibody. We counted the cells in four different retinas and the numbers are 753 ± 29 for WT and 737 ± 59 for MO animals. Range is provided as average ± standard error of the mean. (B) Real time quantitative RT-PCR analysis of four eyes showing that the levels of mRNA are similar in the WT and MO animals. Note the small error bar in the melanopsin only lane.

Supplementary Text

Description of the brain regions innervated by AP labeled ipRGC axons

Suprachiasmatic nucleus

AP-positive axons filled the entire nucleus and extended dorsally at lower density to invade the ventral subparaventricular zone (Fig. 4A, left), just as they did in the *Opn4*$^{tau\text{-}LacZ/+}$ mouse (Fig. 4A, right). However, the staining in the AP mouse was far less uniform within the SCN than in the *Opn4*$^{tau\text{-}LacZ/+}$ mouse. At mid rostrocaudal levels, it was heavily concentrated in comma shaped region occupying the lateral third of the nucleus. This subnuclear organization does not correspond clearly either to the core or to the shell of the nucleus as defined by immunohistochemical markers (Abrahamson and Moore, 2001).

Lateral geniculate nucleus

The most heavily labeled component of the LGN complex was the intergeniculate leaflet (IGL), just as it was in the *Opn4*$^{tau\text{-}LacZ/+}$ mouse (Fig. 4B, left and right). However, the labeling in the ventral division (LGNv) was more intense and widespread than in the *Opn4*$^{tau\text{-}LacZ/+}$ mouse, rivaling that in the IGL in intensity. A particularly striking discrepancy between the two mouse lines was the pattern of fiber labeling within the dorsal division (LGNd). Whereas only a few fibers could be detected in the *Opn4*$^{tau\text{-}LacZ/+}$ mouse, (Fig. 4B, left and right), robust fiber labeling was evident in the *Opn4*$^{Cre/+}$*; Z/AP* line (Fig. 4B, left). As in the *Opn4*$^{tau\text{-}LacZ/+}$ mouse, labeling in the Z/AP mouse comprised only part of the LGNd. Caudally, this labeling was largely restricted to the ventromedial part of the LGNd, but the extent of the labeling grew progressively at more rostral levels, and at the rostral pole of the nucleus filled the cross-section of the nucleus (Fig. 5). The evidence for the dLGN labeling is strong, but is not airtight due to some labeled cells that lack intrinsic light responses. Therefore, doing retrograde injections in the dLGN and recording from the cells that are labeled in the retina should be used to corroborate these results.

Olivary and posterior pretectal nuclei

In the *Opn4*$^{tau\text{-}LacZ/+}$ mouse, the axons of melanopsin-expressing ganglion cells were traced to a region of the pretectum apparently corresponding to the olivary pretectal nucleus (Hattar et al., 2006; Hattar et al., 2002). This terminal zone was comet shaped, with its large head in the

rostromedial pretectum and its tapering tail coursing caudolaterally beneath the rostral superior colliculus to end just lateral to the lateral margin of the colliculus. A striking feature of this terminal field of β-galactosidase-positive afferents was that its rostral head was hollow, forming a 'shell' around a core region that received input from retinal fibers that lacked the marker enzyme (demonstrated clearly in double labeling, Fig. 6B; OPN merged). Other retinorecipient regions of the pretectum were largely free of β-galactosidase positive fibers. Pretectal labeling in the *Opn4*$^{Cre/+}$*; Z/AP* mouse included the olivary pretectal nucleus as marked in the earlier mouse, but differed in two striking ways. First, labeling rostrally included not only the shell of the OPN but its core as well (Fig. 4C, left). In addition, a second elongated band of staining was detectable, paralleling that in the OPN but displaced caudally from it, occupying a region generally designated the posterior pretectal nucleus (PPN) (Fig. 4D, left). In coronal sections through the middle of the pretectal region, this terminal field appeared as an irregularly shaped patch at the dorsomedial margin of the pretectal region. More caudally, it appeared as a complex filigree of labeled patches and wisps sandwiched between the OPN rostrolaterally and the stratum opticum of the superior colliculus caudomedially.

Superior colliculus

Labeling in the superior colliculus (SC) of the *Opn4*$^{Cre/+}$*; Z/AP* mouse was substantially more intense than we had observed in the *Opn4*$^{tau\text{-}LacZ/+}$ mouse. By far the heaviest labeling was in the stratum opticum (SO), especially within the medial and lateral parts of this layer. The SO, the deepest of the superficial visual layers of the colliculus, represents in part the caudal continuation of the optic tract, and is packed with retinofugal fibers coursing caudally to reach their termination in the superficial layers. This may account for some of the labeling in that layer observed here. However, terminal labeling in the overlying superficial gray was surprisingly sparse, suggesting that the stratum opticum is likely to be the layer in which most AP-positive axons terminate, and not merely a conduit for axons en route to the superficial gray layer. Baver et al. (2008) report that M2 ipRGCs lack projections to the colliculus; if so, the heavy labeling of the stratum opticum may derive from the alpha-like or smaller-field, bushier ipRGCs identified in this study.

Other nuclei

Several other targets of melanopsin-expressing RGCs identified in the *Opn4*$^{tau\text{-}LacZ/+}$ mouse were evident in the new mouse line as well. The peri-supraoptic nucleus clearly contained terminal labeling. Several minor forebrain limbic targets identified in the earlier reporter mouse were impossible to evaluate here due to masking by the non-retinal neuronal labeling noted above; these targets included the preoptic nuclei, bed nucleus of the stria terminalis, anterior and lateral hypothalamus and amygdala. The nuclei of the accessory optic system and its pretectal affiliate, the nucleus of the optic tract, appeared to be devoid of fiber labeling in both mouse lines.

Supplementary Experimental Procedures

Details on the generation of animal models, antibody staining, intracellular dye injections and OptoMotry are provided below.

Generation of the mouse models utilized in this study

To generate *Opn4*^{Cre} mice, we used the targeting arms and general strategy detailed in Hattar *et al.*, 2002. The construct contained a 4.4 kb region immediately 5' of the start codon for mouse melanopsin, followed by a human β-globin intron, nuclear localization signal, and Cre recombinase. An FRT-flanked pgk-neomycin resistance cassette was inserted in reverse orientation after the Cre coding region, and preceded the 3' homologous arm consisting of 654 base pairs of melanopsin exon 9 and 946 base pairs beyond this final exon. This FRT flanked region was later excised by mating to Rosa26-flippase mice (see below). Following electroporation and selection with neomycin, mouse embryonic stem cell clones were screened by PCR and Southern blotting to verify proper genomic insertion. PCR was performed using Platinum *Taq* polymerase (Invitrogen) with the following primers: forward primer, 5'- CAC TTG TGT AGC GCC AAG TGC -3'; reverse primer, 5'- TCC TAC ATC CCG AGA TCC AGA CTG -3'. The forward primer was located inside the neomycin resistance gene, and the reverse primer was downstream of the 3' homologous arm. This yielded a roughly 2 kb band from clones that had undergone homologous recombination of the construct. To perform Southern blotting, embryonic stem cell DNA was digested with *Kpn* I (New England Biolabs) and transferred to a Hybond xL membrane (Amersham). The 649 bp Southern probe (the first 92 bp of which overlapped the 3' arm of the construct) was labeled with ^{32}P-dATP and hybridized to the membrane to produce a 6926 bp wildtype band and a 4020 bp mutant band. Chimeras resulting from injection of positive clones were mated to obtain germline transmission, then crossed to mice containing flippase (JAX Mice stock number 003946, *Gt(ROSA)26Sor*$^{tm1(FLP1)Dym}$) to remove the neomycin cassette. They were further bred to remove the flippase gene and to obtain homozygosity for the Cre allele. The experimental animals used in this study were obtained by mating *Opn4*$^{Cre/Cre}$ mice to mice heterozygous for the Z/AP, Z/EG or Brainbow transgenes. The offsprings all possessed a single allele of the melanopsin gene (*Opn4*), which is sufficient to retain intrinsic photosensitivity in ipRGCs (Lucas et al., 2003). To

visualize cells with functional Cre expression, homozygous *Opn4*^{Cre} mice were mated to three reporter lines: Z/AP, Z/EG and Brainbow-1.0. The Z/AP and Z/EG reporter lines are driven by the β-actin/CMV promoter and contain a floxed β-galactosidase/neomycin cassette and STOP sequence that can be excised by Cre-mediated recombination (Fig. S1C and D). This triggers expression of the reporter protein in Cre-expressing cells: placental alkaline phosphatase in *Opn4* $^{Cre/+}$*;Z/AP* (Lobe et al., 1999), and enhanced green fluorescent protein (EGFP) in the Z/EG line (Novak et al., 2000). The Brainbow-1.0 reporter is driven by Thy-1 promoter and upon Cre mediated recombination expresses membrane bound forms of either CFP or YFP (Fig. S1E). The *Opn4*$^{tau\text{-}LacZ/Cre}$*; Brainbow 1.0* animals did not have any copies of the melanopsin gene since both the tau-LacZ and the cre genes replace the melanopsin gene (knock in).

Intracellular dye filling

Single EGFP-labeled retinal ganglion cells were labeled by intracellular dye filling by Lucifer Yellow as described elsewhere (Pu et al., 1994). The areas of cell bodies and dendritic arbors were measured using ImageJ software ((W. Rasband; http://rsb.info.nih.gov/ij/) by fitting a minimal convex polygon their profiles. These were converted to equivalent diameters corresponding to the diameter of the circle having the same areas as the fitted polygon.

Antibody staining

Tissue was fixed by intracardial perfusion with 20 mL 4% paraformaldehyde, followed by immersion fixation of isolated eyeballs in 4% paraformaldehyde for an additional 10 minutes. Eyes were cryoprotected in sterile 30% sucrose in phosphate buffer, then frozen in cryomolds in O.C.T. Compound (Tissue-Tek). Sections were cut at 20 μm with a cryostat, dried for several hours, and were post-fixed for 20 minutes in 4% paraformaldehyde. They were then blocked for 1 hour in phosphate buffer containing 0.3% Triton X-100, 2.5 % heat-inactivated goat serum (Invitrogen), and 2.5% heat-inactivated donkey serum (Chemicon); then stained for three days in primary antibody at 4°C. Secondary incubation was performed for 2 hours at room temperature in the dark. Tissue was mounted in Vectashield fluorescence mounting medium (Vector Laboratories) and viewed under a Zeiss Axio Imager.M1 microscope. Antibody dilutions were as follows: sheep anti-placental alkaline phosphatase, 1:200 (American Research Products, Inc.); rabbit anti-melanopsin, 1:2000 (UF006 from I. Provencio); chicken anti-green fluorescent

protein, 1:1000 (AbCam); goat anti-rabbit AlexaFluor 546, 1:600 (Invitrogen); donkey anti-sheep 488/FITC, 1:600 (Sigma); donkey anti-chicken 488/FITC, 1:600 (Millipore).

For cFos staining in the cortex: brain sections were incubated overnight in primary antibody (Calbiochem Ab-5; 1:20,000 in 0.1M phosphate buffer with 0.5% BSA and 3% Triton X-100) and developed with a Vectastain HRP kit (Vector Labs, Burlingame, CA) and DAB (Metal Enhanced DAB substrate kit, Thermo Scientific, Rockford, Il). Sections were mounted on microscope slides, dehydrated, and coverslipped.

OptoMotry

Unrestrained animals were placed on an elevated platform at the epicenter of the arena where they were allowed to move freely. An experimenter used a video image of the arena from above to view the animal and follow the position of its head with the aid of a computer mouse and a cross-hair superimposed on the video frame. The X-Y positional coordinates of the cross-hair centered the hub of the virtual cylinder, enabling its wall to be maintained at a constant 'distance' from the animal's eyes, thereby fixing the spatial frequency of the stimulus at the animal's viewing position. When the cylinder was rotated and the animal followed with head and neck movements that tracked the rotation, it was judged that the animal's visual system could distinguish the grating.

Homogeneous gray was projected on the cylinder at the beginning of each testing session. The experimenter waited until the animal stopped walking or grooming, at which time gray was replaced with a low spatial frequency (0.04-0.10 cycles/degree (c/d)), high contrast sine wave grating of the same mean luminance, drifting in one direction. The animal was assessed for tracking behavior for a few seconds, and then the gray stimulus was restored. This procedure was repeated until unambiguous examples of tracking were observed. If tracking was observed at low spatial frequencies, the spatial frequency of the grating was increased incrementally, until it was judged that the animal no longer tracked. The process was repeated at least three times for each direction until the highest spatial frequency that elicited tracking was established, which was adopted as the threshold. All experiments were conducted using a cylinder rotation rate of 12°/sec, which is the most favorable speed to judge optokinetic tracking across varying spatial frequencies.

References:

Abrahamson, E.E., and Moore, R.Y. (2001). Suprachiasmatic nucleus in the mouse: retinal innervation, intrinsic organization and efferent projections. Brain Res *916*, 172-191.

Pu, M., Berson, D.M., and Pan, T. (1994). Structure and function of retinal ganglion cells innervating the cat's geniculate wing: an in vitro study. J Neurosci *14*, 4338-4358.